ISSN 1392–1320 MATERIALS SCIENCE (MEDŽIAGOTYRA). Vol. 23, No. 1. 2017

Refinement Strengthening of AZ31 Magnesium Alloy by Warm Constrained Groove Pressing

Peng LIN [1, 2] *, Tingting TANG [1], Zhuoshuai ZHAO [1], Wenxian WANG [1, 2], Chengzhong CHI [1, 2]

[1] *College of Materials Science and Engineering, Taiyuan University of Technology, Taiyuan 030024, PR China*
[2] *Shanxi key laboratory of advanced magnesium-based materials, Taiyuan University of Technology, Taiyuan 030024, PR China*

crossref http://dx.doi.org/10.5755/j01.ms.23.1.14392

Received 16 March 2016; accepted 2 September 2016

The grain refinement and its effect on the mechanical properties of AZ31 magnesium alloys were investigated. The grain refinement was conducted using one of the severe plastic deformation methods, warm constrained groove pressing (CGP) technology. The effective strain was analyzed using the DEFORM-3D software. It was found that the effective strain distribution in AZ31 sheet was homogeneous after a complete four-stage of CGP at 473 K. The average grain size was reduced from 20 μm to 9 μm and the hardness was improved from 55.84 HBW to 69.16 HBW after a complete CGP process at 473 K. The yield stress and ultimate tensile strength increase with grain refinement, from 132 MPa and 240 MPa to 155 MPa and 285 MPa, respectively, following the Hall-Petch relationship. Subjected to annealing at 530 K for 15 minutes, the average grain size of CGP sample decreases slightly and the elongation increased up to 16.2%, close to 17.72% for the pre-CGP samples.

Keywords: constrained grooved pressing, AZ31 magnesium alloys, grain refinement, refinement strengthening.

1. INTRODUCTION

Magnesium alloys have attracted much attention recently due to their low density. However, they exhibit low formability and poor mechanical properties due to their hexagonal closest packed (HCP) structure. As well it is documented, that the strength of the alloy can be improved by grain refinement, following the famous Hall-Petch relationship [1 – 2].

Severe plastic deformation has been widely employed to refine grains in metals and alloys, which improves their mechanical properties accordingly. Equal channel angular pressing (ECAP) [3, 4] and severe torsion straining (STS) [5] have been widely applied to refine grain structure in bulk metals and alloys. However, they both cannot be used for sheet materials. Accumulative roll bonding (ARB) [6 – 8] and repetitive corrugation and straightening (RCS) [9, 10] methods have been employed to process sheet materials. However, the surface requirements are critical for ARB and if the processed sheets are not bonded correctly, the bonding interface may degrade the mechanical properties [7, 8]. For the RCS, the elongation cannot be totally avoided during processing, which will cause strain inhomogeneity in the processed sheets [9, 10]. The elongation, however, can be totally avoided for the sheets during constrained groove pressing (CGP) [11].

The constrained groove pressing (CGP) method, originally proposed by Shin et al [12], was based on the repetitive corrugation and straightening of the sheets and it can produce plate-shaped ultrafine grained metals with relatively homogeneous strain in the sheets. The CGP method has been employed to refine grains for pure aluminum [12, 13], pure Cu [14, 15], Cu-38Zn alloy [16], low carbon steel [17, 18] and nickel sheets [19]. Until now, most researches on CGP were concentrated on metals with face and body centered cubic structure. Few researches aimed at HCP-structure metals. Very recently, the role of biomineralization of AZ31 magnesium alloys was explored using CGP [20].

The aim of this study is to refine magnesium alloy sheets to improve their mechanical properties using warm CGP method. The effect of CGP on microstructure and mechanical properties of the AZ31 Mg alloy sheet was investigated.

2. EXPERIMENTAL PROCEDURE

2.1. Material

The nominal compositions of the AZ31 magnesium alloy used in the present study are 2.9wt.% Al, 0.88wt.% Zn, 0.2wt.% Mn and the rest is Mg. The as-received AZ31 plates with dimensions of 44×44×2 mm were annealed at 550 K for 1 h before CGP process, termed as pre-CGP samples in the present study.

2.2. Constrained groove pressing

The process of CGP is illustrated in Fig.1, where the sample direction is also indicated. A complete CGP pass contains four stages. As Fig.1a shows, a series of grooves were machined in the upper and bottom dies, where the depth of these grooves are equal to those of the slope width, resulting in a 45° lope for the groove wall. For the assembly, the grooves of upper and bottom are asymmetry, as Fig. 1 a shows. The thickness of the processed sheet has no change during CGP.

*Corresponding author: Tel: +86-0351-6010021.
E-mail address: *linpengtyut@hotmail.com* (P. LIN)

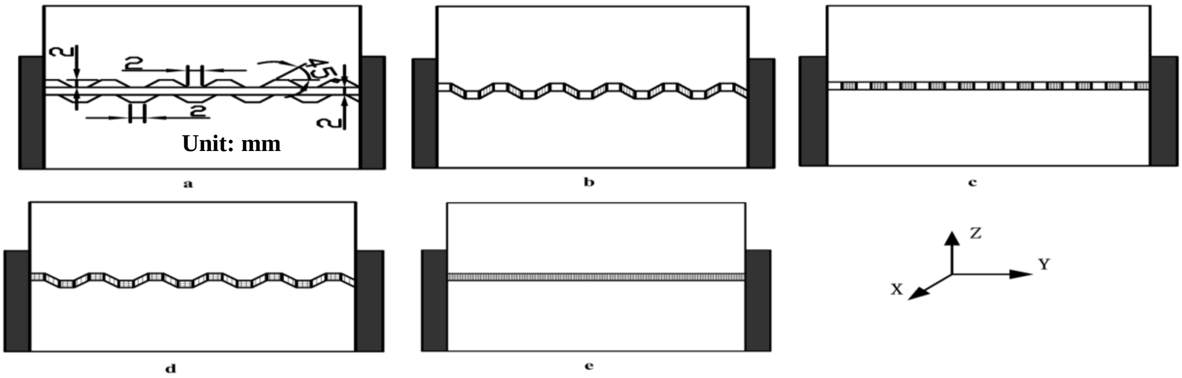

Fig. 1. Schematic illustration of the CGP process: a – the initial set up; b – after the first stage; c – after the second stage; d – the AZ31 sheet was rotated by 180°, and then was pressed for the third stage; e – after the fourth stage

After the first stage, the sheet corresponding to the slope of the groove wall is subjected to pure shear deformation, resulting in a certain effective strain (single hatched region in Fig. 1 b), while the flat part of the sheet has not experienced any deformation (unhatched region in Fig. 1 b).The second stage of CGP is flatting the corrugated sheet. In this stage, the deformed regions are subjected to a reverse shear deformation, double the effective strain in the first stage (double hatched area in Fig. 1 c). However, the un-deformed region in the first stage remains un-deformed. After the second stage, the processed sheet was rotated by 180°, which allows the un-deformed region to be deformed in the following pressing due to the asymmetry of the grooved dies. The stage 3 and 4 are similar to stage 1 and 2, and the difference between them is the deformation regions. After four-stage of processing, the produced sheet is flat, resulting in a homogeneous effective strain in the whole processed sheet (Fig. 1 e).

In the present study，the CGP was conducted using a DNS 200 electronic pressing machine operating at a strain rate of 0.01 s^{-1} at 473 K. The samples experienced the whole CGP were marked as the post-CGP samples. Some of them were subsequently annealed at 530 K for 15 minutes, termed as post-CGP plus annealed samples.

The homogeneity of the samples was evaluated using a THB-3000 Electronic Brinell hardness tester with a 62.5 kg load for 30 s along Y direction of the samples (as indicated in Fig. 1). Five measurements were conducted for each sample with a pitch distance of 6 mm.

The mechanical properties of the samples were conducted at room temperature along Y direction using a DNS 200 electronic testing machine. The tensile testing specimens were machined with a gage length of 15×3.5 mm^2.

The microstructure and grain size of samples were characterized using Leica DM2700M optical microscope. The samples were ground using SiC paper up to 2000# and then polished and cleaned using the mixture of 90 vol.% alcoholic and 10 vol.% water. To reveal the grain structure, the polished samples were etched using a mixture of 4.2 g $C_6H_3N_3O_7$ 20 ml H_2O, 10 ml CH_3COOH, and 70 ml C_2H_5OH for 10 seconds. The grain size was measured using linear interception method for at least 100 grains from each direction (X or Y direction, as indicated in Fig. 1) for each sample.

2.3. Finite element analysis

The commercial finite element software, DEFORM-3D, is applied to investigate deformation behavior and effective-strain distribution in the post-CGP samples. Both flat and grooved dies were assumed to be discrete rigid during simulation. The upper die speed was kept a constant of 0.034 mm/s, the same as that of the experimental process. The true stress-strain relationship of the annealed sheet at 473 K was imported to the software. Adaptive meshing, mass scaling and automatic re-meshing were applied and justified for all of the simulations to prevent failure of the mesh during large deformation and to reduce computation time. Mesh sensitivity was performed and the optimum element size was found. Eighty thousand meshes were selected in the present study.

3. RESULTS AND DISCUSSION

3.1. Theoretical analysis

The processed sheet was under plane strain deformation on YOZ plane (Fig.1) during CGP due to the shear strain in each stage. Therefore,

$$\gamma_{xy} \approx \tfrac{1}{2}\tan\alpha = \tfrac{1}{2}(\alpha = 45^{\circ}), \quad (1)$$

where α is the die angle, γ_{xy} is the shear strain.

The effective-strain can be calculated by:

$$\varepsilon_{\varepsilon ff} = \frac{\sqrt{3}}{2}\sqrt{6\gamma_{xy}^{2}} = \frac{\sqrt{3}}{3}, \quad (2)$$

where $\varepsilon_{\varepsilon ff}$ is the effective-strain, γ_{xy} is the shear strain.

The result of the finite element analysis on the distribution of effective strain of the sheet after the first stage is shown in Fig. 2.

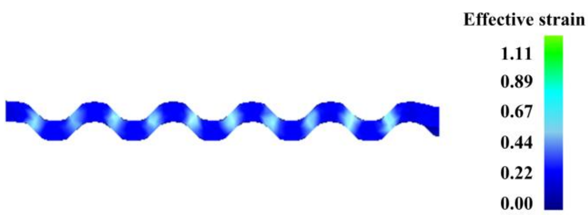

Fig. 2. The simulated effective strain after the first stage of CGP process using DEFORM-3D software

The corrugated region was presented using light blue color while the straight region was indicated using dark blue color. As shown, the corrugated region has a large effective strain, close to 0.58, while the straight region has very limited strain, nearly 0.

Fig. 3 a presents the effective strain variation along X direction. It has limited fluctuation at around the theoretical value of 0.58, which is consistent with the literature [21]. The effective strain of the first and the last points have a variation compared to the point in the center. It might be related to the locations of the two points, where a complex stress/strain is imposed on the processed sheet. Fig. 3 b presents the effective strain variation along Y direction. The effective strain has limited fluctuation at around the theoretical strain of 0.58 as well.

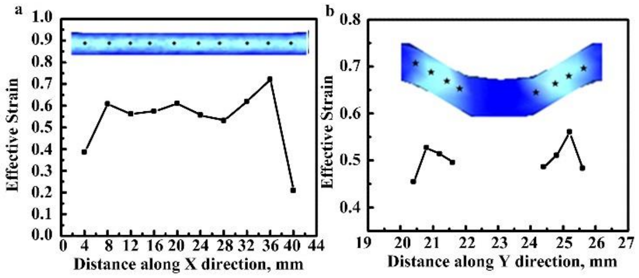

Fig. 3. The effective strain after the first stage of CGP process: a – along X direction; b – along Y direction

3.2. Microstructure

The microstructure of the AZ31 magnesium alloy sheet are shown in Fig. 4. The pre-CGP sample has an average size of 20.7 ± 0.71 μm along X and 19.8 ± 0.70 μm along Y direction. So, the sheet has a near equiaxed grain structure for the pre-CGP samples (Fig. 4 a). After a complete CGP pass, the grain size is reduced to around 9.8 ± 5.57 μm along X and 8.8 ± 4.61 μm along Y directions (Fig. 4 b). After annealing at 530 K for 15 minutes, the grain size has a little increment, at around 10.8 ± 5.35 μm along X and 9.97 ± 2.26 μm along Y direction (Fig. 4 c). In this case, the grain size variation is between 4.0 μm and 14.6 μm, whose range decreases significantly compared to that from the post-CGP samples. Additionally, a lot of small grains can be observed at the grain boundaries of coarse grains, as Fig. 4 b shows, impling that dynamic recrystallization took place during the CGP pressuring. Therefore, the mechanism of grain refinement using CGP method should be continuous dynamic recovery and recrystallization (CDRR) process [22].

Moreover, the deformation twining can be found in the CGP processed samples, as Fig. 4 b and c shown, indicating the AZ31 Mg alloy sheet deformed mainly through dislocations glide and the deformation twinning assists the activation of secondary slip systems. The grain size variation implies that the deformation is in-homogeneous in micro scale, although the alloy experienced an overall homogeneous effective strain after a series of CGP. As stated above, only one complete CGP process was conducted for the AZ31 sheet. The issue of grain size variation should be further investigated in the future with a series of continuous CGP processes.

3.3. Mechanical properties

3.3.1. Tensile property

The stress-strain relationships of the AZ31 Mg alloy before and after CGP are shown in **Fig.5a**. After CGP, the ultimate tensile strength was improved from 240 MPa to 285 MPa and the elongation decreased from 17.72% to 12.29%. Subjected to annealing at 530 K for 15 minutes, the ultimate tensile strength decreased a little bit while the elongation increased significantly up to 16.2%, which is comparable with that of pre-CGP samples. Therefore, the annealing treatment increases significantly the elongation while the ultimate tensile strength decreases slightly.

The effect of grain refinement is attributed to the famous Hall-Petch relationship.

$$\sigma_s = \sigma_0 + k_y d^{-1/2}, \tag{3}$$

where σ_0 and k_y are the material constants and d is the grain size. When the grains were refined by CGP, the yield stress was improved from 132 MPa to 155 MPa. Fig. 5 b presents the experimental data of yield stress and reciprocal square root of grain size, where a straight relation is obtained with a slope of 188.6. Therefore, the grain refinement of the AZ31 Mg alloy follows Hall-Petch relationship. This is related to the dislocation pile-ups and the deformation twinning formation during CGP processes.

3.3.2. Hardness distribution

To characterize the mechanical property homogeneity of the CGP processed AZ31 Mg alloy sheet, hardness was tested along Y direction at 5 points with a pitch length of 6 mm.

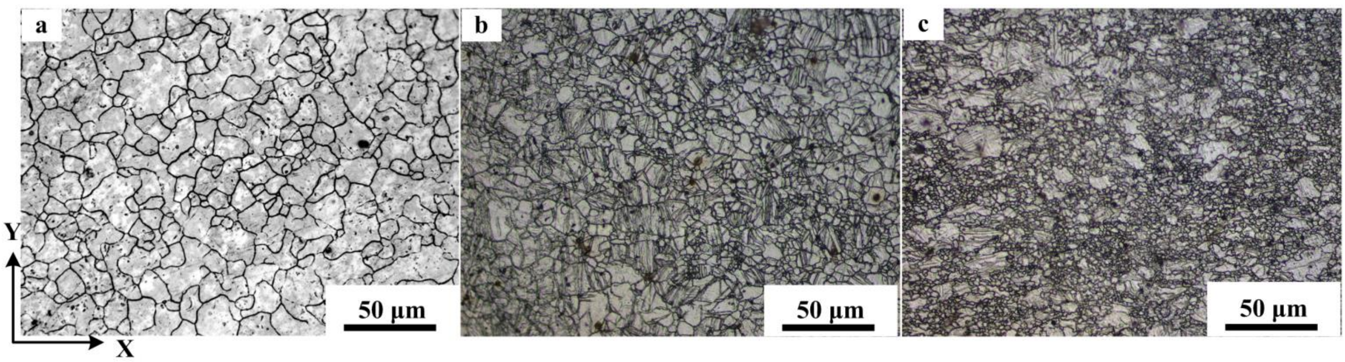

Fig. 4. The microstructure of AZ31 Mg alloy sheet: a – pre-CGP sheet; b – post-CGP sheet; c – post-CGP plus annealed CGP sheet at 530 K for 15 minutes

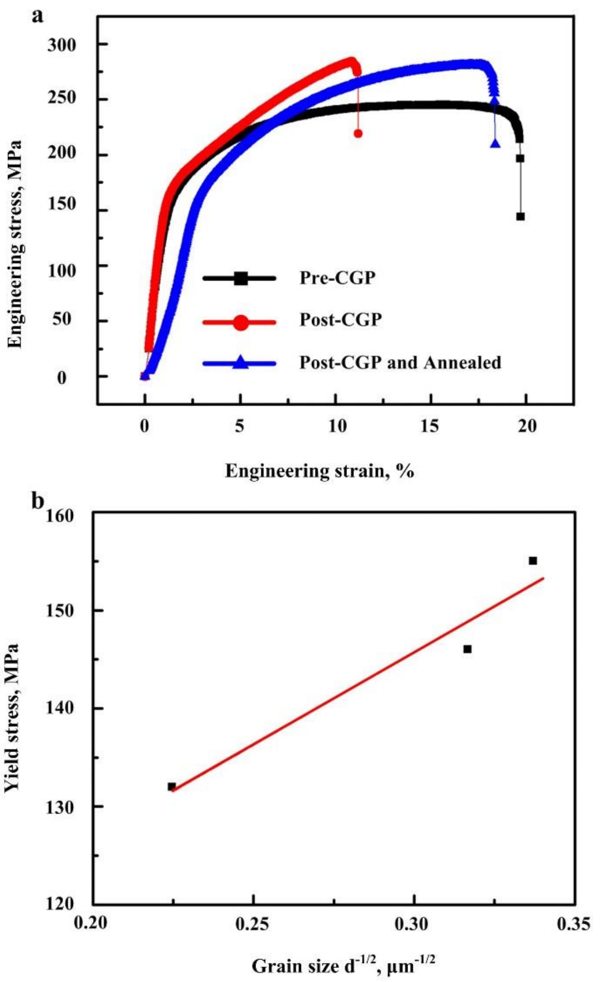

Fig. 5. a – stress-strain curves and b – the yield strength variation versus grain size of $d^{-1/2}$ of AZ31 Mg alloys of pre-CGP, post-CGP, and post-CGP plus annealed sheets at 530 K for 15 minutes

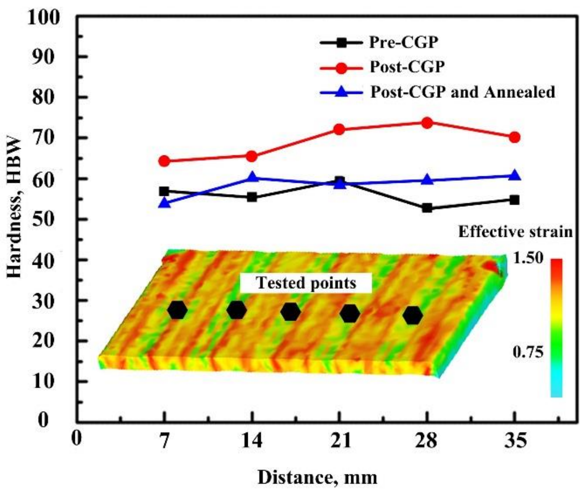

Fig. 6. Hardness distribution along Y direction of AZ31 Mg alloy sheet, and the inset picture schematically shows the testing points

This experimental design can cover both the sheared and non-deformed region after the first-stage of CPG process. Fig. 6 presents the test results from pre-CGP, post-CGP, and post-CGP plus annealed sheets at 530 K for 15 minutes. First of all, the hardness of AZ31 Mg alloy sheet was increased by CGP from 55.84 ± 2.50 HBW to 69.16 ± 4.17 HBW, with a increment of about 23 %. After annealing at 530 K for 15 minutes, the hardness decreased to about 58.48 ± 2.74 HBW, which is slightly higher than that of pre-CGP samples. This trend is consistent with the tensile properties, as Fig. 5 shows. Additionally, the measured hardness value shows some fluctuation for each sample, and the fluctuation is largest for the post-CGP sample. From the hardness results, it is reasonable to conclude that the mechanical properties of CGP processed sheets is homogeneous in macro scale. However, from micro scale, the CGP processed AZ31 Mg alloy sheet is in-homogeneous, as Fig. 4 shows. This discrepancy is related to the characterization method difference. For hardness measurement, the deformation region can be in millimeter scale or even larger. Therefore, the hardness represents the average properties of a local region. However, measured grain size is in the range of 1 ~ 20 μm. Thus, one hardness value represents the average properties of a bunch of grains.

The present study provides a simple method to refine HCP-structured metal and alloys, like AZ31 Mg alloys, using CGP technology. With only one complete CGP processing, the average grain size is reduced around 50% for AZ31 Mg alloys. It is expected that the grain size can be further refined and homogenized with multiple CGPs. Accordingly, the mechanical properties can be improved following the Hall-Petch relationship.

4. CONCLUSIONS

The grain refinement of AZ31 Mg alloy sheet was conducted using CGP method in the present study, and the effect of grain refinement on the mechanical properties was studied. The main findings include:

1. CGP is a useful method to refine grains of AZ31 Mg alloy sheets. After four stages of CGP processes, the sheet is homogeneous in macro scale along both X and Y directions. The effective strain is 0.58 for each stage.
2. The average grain size of the AZ31 Mg alloy sheet can be refined from 20 μm to 9 μm after one complete CGP process at 473 K. After CGP process, some small grains formed at the grain boundaries of coarse grains due to dynamic recrystallization. With further annealing, the homogeneity increases although the average grain size increases from 9 μm to 10 μm.
3. The yield strength and ultimate tensile strength of AZ31 magnesium alloys increase with grain refinement, from 132 MPa and 240 MPa to 155 MPa and 285 MPa, respectively, following the Hall-Petch relation. Subjected to annealing at 530 K for 15 minutes, the ultimate tensile strength decreased a little while the elongation increased significantly up to 16.2 %, comparable with that of pre-CGP sheets.

Acknowledgments

This work was supported by National Natural Science Foundation of China under grant No.51505323 and No. 51375328.

REFERENCES

1. **Fatemi-Varzaneh, S.M., Zarei-Hanzaki, A., Izadi, S.** Shear Deformation and Grain Refinement during Accumulative Back Extrusion of AZ31 Magnesium Alloy *Journal of Materials Science* 46 (6) 2011: pp. 1937 – 1944. https://doi.org/10.1007/s10853-010-5029-8
2. **Yu, X., Li, Y., Li, L.** Effect of Grain Refinement on Fracture Toughness and Fracture Mechanism in AZ31 Magnesium Alloy *Procedia Materials Science* 3 2014: pp. 1780 – 1785.
3. **Iwahashi, Y., Wang, J., Horita, Z. Nemoto, M., Langdon,T.G.** Principle of Equal-Channel Angular Pressing for the Processing of Ultra-Fine Grained Materials *Scripta Materialia* 35 (2) 1996: pp. 143 – 146.
4. **Xia, K., Wang, J.T., Wu, X., Chen, G., Gurvan, M.** Equal Channel Angular Pressing of Magnesium Alloy AZ31 *Materials Science & Engineering A* 410 (12) 2005: pp. 324 – 327. https://doi.org/10.1016/j.msea.2005.08.123
5. **Nakamura, K., Neishi, K., Kaneko, K., Nakagaki, M., Horita, Z.** Development of Severe Torsion Straining Process for Rapid Continuous Grain Refinement *Materials Transactions* 45 (12) 2004: pp. 3338 – 3342.
6. **Kamikawa, N., Tsuji, N., Minamino, Y.** Microstructure and Texture Through Thickness of Ultralow Carbon if Steel Sheet Severely Deformed by Accumulative Roll-Bonding *Science & Technology of Advanced Materials* 5 (1 – 2) 2016: pp. 163 – 172.
7. **Saito, Y., Utsunomiya, H., Tsuji, N., Sakai, T.** Novel Ultra-High Straining Process for Bulk Materials-Development of the Accumulative Roll-Bonding (ARB) Process *Acta Materialia* 47 (2) 1999: pp. 579 – 583. https://doi.org/10.1016/S1359-6454(98)00365-6
8. **Saito, Y., Tsuji, N., Utsunomiya, H., Sakai, T., Hong, R.G.** Ultrafine Grained Bulk Aluminum Produced by Accumulative Roll-Bonding (ARB) Process *Scripta Materialia* 39 (9) 1998: pp. 1221 – 1227. https://doi.org/10.1016/S1359-6462(98)00302-9
9. **Huang, J.Y., Zhu, Y.T., Jiang, H., Lowe, T.C.** Microstructures and Dislocation Configurations in Nanostructured Cu Processed by Repetitive Corrugation and Straightening *Acta Materialia* 49 (9) 2001: pp. 1497 – 1505.
10. **Huang, J., Zhu, Y.T., Alexander, D.J., Liao, X., Lowe, T.C., Asaro, R.J.** Development of Repetitive Corrugation and Straightening *Materials Science & Engineering A* 371 (1 – 2) 2004: pp. 35 – 39.
11. **Hosseini, E., Kazeminezhad, M., Mani, A., Rafizadeh, E.** On the Evolution of Flow Stress During Constrained Groove Pressing of Pure Copper Sheet *Computational Materials Science* 45 (4) 2009: pp. 855 – 859.
12. **Dong, H.S., Park, J.J., Kim, Y.S., Park, K.T.** Constrained Groove Pressing and its Application to Grain Refinement of Aluminum *Materials Science & Engineering A* 328 (1 – 2) 2002: pp. 98 – 103.
13. **Morattab, S., Ranjbar, K., Reihanian, M.** On The Mechanical Properties and Microstructure of Commercially Pure Al Fabricated by Semi-Constrained Groove Pressing *Materials Science & Engineering A* 528 (22 – 23) 2011: pp. 6912 – 6918.
14. **Krishnaiah, A., Chakkingal, U., Venugopal, P.** Applicability of the Groove Pressing Technique for Grain Refinement in Commercial Purity Copper *Materials Science & Engineering A* 410 (12) 2005: pp. 337 – 340.
15. **Rafizadeh, E., Mani, A., Kazeminezhad, M.** The Effects of Intermediate and Post-Annealing Phenomena on the Mechanical Properties and Microstructure of Constrained Groove Pressed Copper Sheet *Materials Science & Engineering A* 515 (1 – 2) 2009: pp. 162 – 168.
16. **Peng, K., Zhang, Y., Shaw, L.L., Qian, K.W.** Microstructure Dependence of a Cu-38Zn Alloy on Processing Conditions of Constrained Groove Pressing *Acta Materialia* 57 (18) 2009: pp. 5543 – 5553.
17. **Khodabakhshi, F., Kazeminezhad, M.** The Effect of Constrained Groove Pressing on Grain Size, Dislocation Density and Electrical Resistivity of Low Carbon Steel *Materials & Design* 32 (6) 2011: pp. 3280 – 3286.
18. **Shadmehri, M., Khajenabi, F.** The Annealing Phenomena and Thermal Stability of Severely Deformed Steel Sheet *Materials Science & Engineering A* 528 (528) 2011: pp. 5212 – 5218.
19. **Kumar, S.S.S., Raghu, T.** Mechanical Behaviour and Microstructural Evolution of Constrained Groove Pressed Nickel Sheets *Journal of Materials Processing Technology* 213 (2) 2013: pp. 214 – 220.
20. **Sunil, B.R., Kumar, A.A., Kumar, T.S.S., Chakkingal, U.** Role of Biomineralization on the Degradation of Fine Grained AZ31 Magnesium Alloy Processed by Groove Pressing *Materials Science & Engineering C* 33 (3) 2013: pp. 1607 – 1615.
21. **Sajadi, A., Ebrahimi, M., Djavanroodi, F.** Experimental and Numerical Investigation of Al Properties Fabricated by cgp Process *Materials Science & Engineering A* 552 (552) 2012: pp. 97 – 103. https://doi.org/10.1016/j.msea.2012.04.121
22. **Jin, L., Lin, D., Mao, D., Zeng, X., Chen, B., Ding, W.** Microstructure Evolution of AZ31 Mg Alloy during Equal Channel Angular Extrusion *Materials Science & Engineering A* 423 (1) 2006: pp. 247 – 252. https://doi.org/10.1016/j.msea.2006.02.045